High-peak-power passively *Q*-switched Nd:YAG/Cr^{4+}:YAG composite laser with multiple-beam output

T. Dascalu, G. Croitoru, O. Grigore, and N. Pavel*

National Institute for Laser, Plasma and Radiation Physics, Laboratory of Solid-State Quantum Electronics, Magurele, Ilfov, Bucharest 077125, Romania
**Corresponding author: nicolaie.pavel@inflpr.ro*

Received July 26, 2016; revised September 25, 2016; accepted September 26, 2016; posted September 28, 2016 (Doc. ID 272440); published October 21, 2016

We report on the design, realization, and output performance of a diode-pumped high-peak-power passively *Q*-switched Nd:YAG/Cr^{4+}:YAG composite medium monolithic laser with four-beam output. The energy of a laser pulse was higher than 3 mJ with duration of 0.9 ns. The proposed system has the ability to choose independently the focus of each beam. Such a laser device can be used for multipoint ignition of an automobile gasoline engine, but could also be of interest for ignition in space propulsion or in turbulent conditions specific to aeronautics.

OCIS codes: (140.3580) Lasers, solid-state; (140.3530) Lasers, neodymium; (140.3540) Lasers, *Q*-switched; (140.5560) Pumping.
http://dx.doi.org/10.1364/PRJ.4.000267

1. INTRODUCTION

Ignition induced by laser is currently viewed as an alternative technique to ignition realized by a spark plug, especially for vehicles with internal combustion engines [1–4]. Among the advantages of this new ignition method, one could mention: (i) the absence of the quenching effect of the developing flame kernel due to the lack of a spark plug electrode, resulting in a shorter burn duration; (ii) the possibility to ignite at an optimal position into the engine chamber for efficient combustion; (iii) lowering fuel consumption and decreasing exhaust gas emissions under conditions of normal engine operation, i.e., near the stoichiometric air–fuel ratio, or (iv) the possibility to ignite lean air–fuel mixtures and thus to further reduce engine impact on the environment.

A CO_2 laser was used to obtain in 1978, for the first time, the ignition by laser of a single-cylinder engine [5]. Furthermore, a four-cylinder engine was ignited, in 2008, by a *Q*-switched Nd:YAG laser [6]. Because of the experimental conditions, the bulky lasers were placed outside of the engines and the laser beams were directed into the engine cylinders by adequate optics.

A solution for realization of a compact spark-like laser device was proposed in 2007 by Kofler *et al.* [7]. Thus, it was shown that a Nd:YAG laser medium that is passively *Q*-switched by a Cr^{4+}:YAG crystal with saturable absorption (SA) can deliver pulses with few-millijoule energy and nanosecond-order duration, suitable for laser ignition. The first high-peak-power passively *Q*-switched Nd:YAG-Cr^{4+}:YAG spark-plug laser was realized in 2010 by Tsunekane *et al.* [8]; furthermore, the same research group has investigated the characteristics of a Yb:YAG-Cr^{4+}:YAG discrete media combination for laser ignition applications [9]. Several other approaches, like the passively *Q*-switched diffusion-bonded Nd:YAG/Cr^{4+}:YAG laser with wedged Cr^{4+}:YAG SA [10] or the diffusion-bonded Nd:YAG/Cr^{4+}:YAG laser pumped laterally through a YAG prism [11], could also be considered and optimized in order to be used for ignition by a laser. It is worth mentioning that the majority of these lasers were pumped longitudinally with fiber-coupled diode lasers. On the other hand, side pumping with a diode array enabled the realization of a high-energy Nd:YAG-Cr^{4+}:YAG laser (the so-called HiPoLas laser) [12]; the same pumping scheme was employed to build a passively *Q*-switched Nd:YAG-Cr^{4+}:YAG pulse-burst laser for laser ignition [13].

For the first time, in 2013 an automobile gasoline engine was ignited with only laser sparks by Taira *et al.* [14]. Recently, we have also operated a four-cylinder engine with laser sparks [15]. Measurements at average speeds (below 2.000 rpm) concluded that ignition by laser improves engine stability and decreases emission of CO and HC in comparison with the same engine that was ignited by classical spark plugs. In these experiments, laser sparks that were built with diffusion-bonded Nd:YAG/Cr^{4+}:YAG composite media and that delivered single-beam output have been used [14,15]. On the other hand, a laser offers the possibility to obtain ignition at multiple points, thus better and more uniform combustion in comparison with ignition by electrical spark plugs. For example, increased pressure and shorter combustion time were measured for laser ignition in two points of CH_4/air and H_2/air mixtures in a static chamber [16]. Also, experiments realized with H_2/air mixtures (in a static chamber) concluded that ignition at two points assures faster combustion in comparison with single-point ignition [17].

To generate multiple points of ignition, several solutions have been proposed. Thus, end pumping with three independent lines of a passively *Q*-switched diffusion-bonded Nd:YAG/Cr^{4+}:YAG composite ceramic medium allowed realization of the first spark-plug-like laser device with three focusing points, at fixed locations [18]. In another approach, a spatial light modulator was applied to a single laser beam to

obtain multipoint laser-induced spark generation with arbitrary geometrical location in three dimensions or at different distances on the central axis of propagation [19]. The energetic beam (with long, 10 ns duration at 1064 nm) was, however, delivered by a flash-lamp-pumped Q-switched Nd:YAG laser. Also, a 2×2 lens array was employed to transfer the pump beam from a fiber-coupled diode laser to a Nd:YAG-Cr^{4+}:YAG laser and thus to realize a device with four-beam output [20]. Each laser beam operated in burst mode, and every pulse burst contained two to five pulses of low (0.12–0.22 mJ) energy and long (10.5–11.5 ns) duration at a kilohertz-order repetition rate. In this case, further increase of the laser pulse energy is necessary to obtain air breakdown.

In this work we report on the design, realization, and performance of a high-peak-power passively Q-switched Nd:YAG/Cr^{4+}:YAG composite monolithic laser that yields four independent beams, each beam having appropriate characteristics for laser ignition. A compact optical system was made to transfer every pump beam into Nd:YAG/Cr^{4+}:YAG, keeping the compactness of the device and assuring millimeter-order distance between laser beams. Typically, the energy of a laser pulse was higher than 3 mJ with duration shorter than 1 ns. The focusing system was designed for various purposes, aiming focusing and air breakdown in four points (in the same plane or at different distances from the laser) or in a single point. This laser can be used for multipoint ignition of an automobile engine; it could be also of interest in space propulsion systems [21,22] or for ignition in turbulent conditions specific to aeronautical combustion [23].

2. THE LASER CONFIGURATION

A. Design: Single Line, Experiments, and Modeling

The laser configuration is shown in Fig. 1. The laser medium is an Nd:YAG/Cr^{4+}:YAG composite structure of 10 mm diameter; it was made of an 8.5 mm long, 1.1 at. % Nd:YAG medium that was bonded to a 2.5 mm thick Cr^{4+}:YAG SA with initial transmission (T_i) of about 40%. Such an Nd:YAG/Cr^{4+}:YAG medium assures robustness and compactness, as well as a high resistance at vibrations of the laser [14,15,18].

A monolithic resonator was obtained by coating the surface S1 of Nd:YAG with a high-reflectivity mirror (HRM, reflectivity

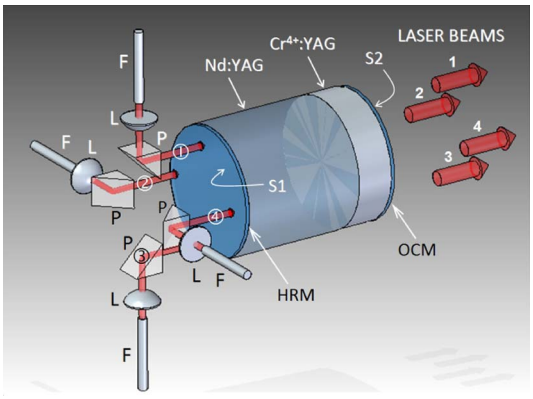

Fig. 1. Laser configuration (patent pending) is shown. Each pump beam (①,②, ③, and ④) is directed from the corresponding optical fiber (F) to the composite Nd:YAG/Cr^{4+}:YAG medium through a lens (L) and a folding prism (P). Four (1, 2, 3, and 4) laser beams are obtained.

$R > 0.999$) at the laser wavelength $\lambda_{em} = 1.06$ μm and the outcoupling mirror (OCM) with transmission $T_{OCM} = 50\%$ (±5%) on surface S2 of Cr^{4+}:YAG. Surface S1 was also coated with a high transmission layer ($T > 0.98$) at the pump wavelength $\lambda_p = 807$ nm. It is worth mentioning that, in this design, the pump-beam absorption efficiency in Nd:YAG was evaluated to be around 0.95. Therefore, the Cr^{4+}:YAG SA properties were not influenced by the residual pump beam. We mention that Nd:YAG/Cr^{4+}:YAG single crystals as well as Nd:YAG/Cr^{4+}:YAG fabricated by ceramic techniques were used in experiments. The best results were obtained with Nd:YAG/Cr^{4+}:YAG ceramic (or polycrystalline) media from Baikowski Co., Japan.

The pump was made at $\lambda_p = 807$ nm with fiber-coupled (diameter of 400 μm and numerical aperture NA = 0.22) diode lasers (JOLD-120-QPXP-2P, Jenoptik, Germany) that were operated in quasi-continuous-wave regime; in the experiments, the pump pulse duration was set at 250 μs and the repetition rate was increased up to 60 Hz. To keep the pump line simple, the pump beam delivered through a fiber (F) was focused into Nd:YAG with only a single lens (L). A small prism (P) was used to fold each pump line and thus to accommodate four fibers around surface S1 of Nd:YAG.

The pump-line configuration was decided first. For this purpose, the Nd:YAG/Cr^{4+}:YAG composite ceramic medium was pumped directly from fiber F with only one lens, L. The distance between F and L was noted by d_1 and the distance from L to the Nd:YAG/Cr^{4+}:YAG was denoted by d_2. Several aspherical lenses L, with focal length f between 3.1 and 7.5 mm were employed; for each lens, the laser pulse energy E_p was measured as a function of d_1 and d_2.

Figure 2(a) shows several results obtained with two lenses, the first with focal length $f = 4.0$ mm and a second one with $f = 6.2$ mm. In these investigations the repetition rate was set at 5 Hz. When the lens with $f = 4.0$ mm was placed at $d_1 = 3.4$ mm from optical fiber F, laser pulses with energy $E_p = 2.9$ mJ were obtained for Nd:YAG/Cr^{4+}:YAG positioned at distance $d_2 = 7.5$ mm [Fig. 2(a)]. The corresponding pump pulse energy was $E_{pump} = 26$ mJ [Fig. 2(b)]. Increasing d_2 at 10 mm improved E_p at 5.2 mJ, whereas E_{pump} reached the level of ~45 mJ. In the case of lens L with $f = 6.2$ mm placed at $d_1 = 4.9$ mm, laser pulses with $E_p = 3.0$ mJ were measured for Nd:YAG/Cr^{4+}:YAG situated at distance $d_2 = 15$ mm; the requested pump pulse energy was $E_{pump} = 31.8$ mJ. For this lens, the laser could be operated up to a distance $d_2 = 18.5$ mm; at this point, the laser pulse energy increased to $E_p = 5.9$ mJ and the available pump energy $E_{pump} = 47$ mJ delivered by the diode was reached. The colored points for E_p shown in Fig. 2(a) were used in modeling (as will be explained below). We have also measured the laser beam M^2 factor using the knife-edge method (10%–90% level, ISO 11146/2005). For laser pulses with energy E_p around 3 mJ (a minimal value of interest for realizing air breakdown in our experimental conditions), the M^2 factor was around 4.1; the beam quality decreases with increasing the laser pulse energy, with M^2 factor of about 5.2 for pulses with $E_p \sim 5$ mJ.

To explain the laser pulse performance, we have applied a model developed in our previous work [15,18]. Thus, we remember that the laser pulse energy can be written by [24,25]

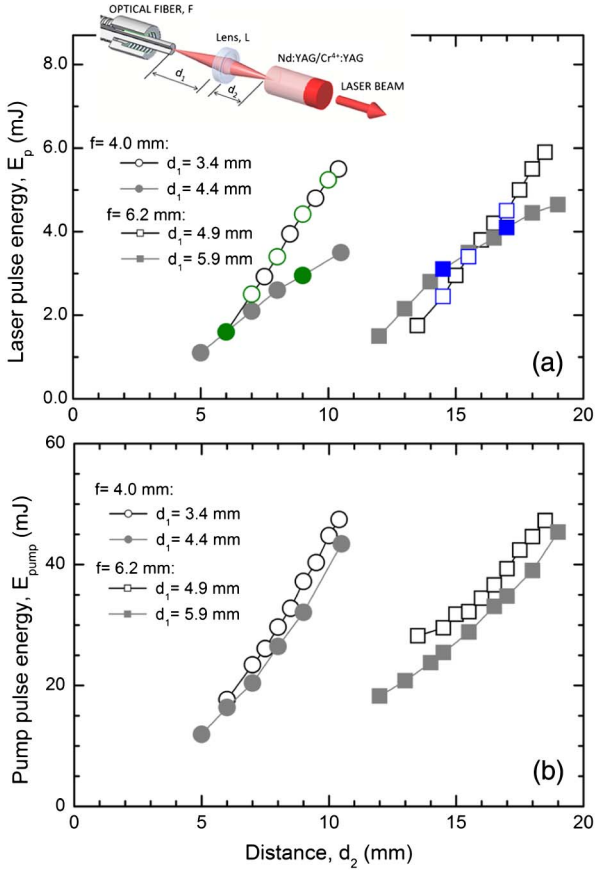

Fig. 2. (a) Laser pulse energy E_p versus distance d_2 between lens L and surface S1 of Nd:YAG. Data for two lenses, first with focal length $f = 4.0$ mm placed at distances $d_1 = 3.4$ and 4.4 mm from F, and the second with $f = 6.2$ mm positioned at $d_1 = 4.9$ and 5.9 mm from F, are shown. The inset is a sketch of the single pump-beam arrangement. (b) The corresponding pump pulse energy, E_{pump}, is plotted.

$$E_p = \frac{h\nu}{2\gamma_g\sigma_g} A_g \times \ln\frac{1}{R_{\text{OCM}}} \times \ln\left(\frac{n_{gf}}{n_{gi}}\right), \tag{1}$$

where $h\nu$ is the photon energy at λ_{em}, γ_g is the inversion factor, and σ_g represents the Nd:YAG emission cross section. A_g is the laser beam cross-section area in Nd:YAG and the OCM reflectivity is $R_{\text{OCM}} = (1 - T_{\text{OCM}})$. The density of the initial inversion of population is $n_{gi} = \beta/(2\sigma_g\lambda_g)$, with λ_g the Nd:YAG length. The density of the final inversion of population n_{gf} was obtained from the transcendental equation [15,18]:

$$(1 - r_n) + \left(1 + \frac{(1-\delta)\times \ln T_i^2}{\beta}\right) \times \ln(r_n) + \frac{1}{\alpha} \times \frac{(1-\delta)\times \ln T_i^2}{\beta} \times (1 - r_n^{\alpha}) = 0, \tag{2}$$

where r_n is the ratio $r_n = n_{gf}/n_{gi}$. The element $\beta = (-\ln R_{\text{OCM}} + L_t - \ln T_i^2)/[1 - \exp(-2a^2)]$ includes the parameter a, defined as the ratio between the pump-beam radius ω_p and the laser-beam radius ω_g in Nd:YAG, $a = \omega_p/\omega_g$. L_t is the double-pass residual loss of the monolithic Nd:YAG/Cr^{4+}:YAG laser, accounting for the Nd:YAG losses (L_i) as well as for the final transmission (T_f) of Cr^{4+}:YAG SA. Also, δ is the ratio $\delta = \sigma_{\text{ESA}}/\sigma_{\text{SA}}$, with σ_{ESA} the excited-state absorption cross section and σ_{SA} the absorption cross section of Cr^{4+}:YAG; α is $\alpha = (\gamma_{\text{SA}}\sigma_{\text{SA}})/(\gamma_g\sigma_g) \times (A_g/A_{\text{SA}})$, with γ_{SA} the inversion reduction factor for Cr^{4+}:YAG. The laser beam area in Cr^{4+}:YAG, A_{SA}, and A_g were considered equal, a fair approximation due to the short length of the Nd:YAG/Cr^{4+}:YAG medium. For the simulations, the Nd:YAG emission cross section was taken as $\sigma_g = 2.63 \times 10^{-19}$ cm^2; the absorption cross section and excited-state absorption cross section of Cr^{4+}:YAG SA were $\sigma_{\text{SA}} = 4.3 \times 10^{-18}$ cm^2 and $\sigma_{\text{ESA}} = 8.2 \times 10^{-19}$ cm^2, respectively. Because of the high value of the M^2 factor, the pump beam as well as the laser beams were considered to have uniform (like top-hat) distributions.

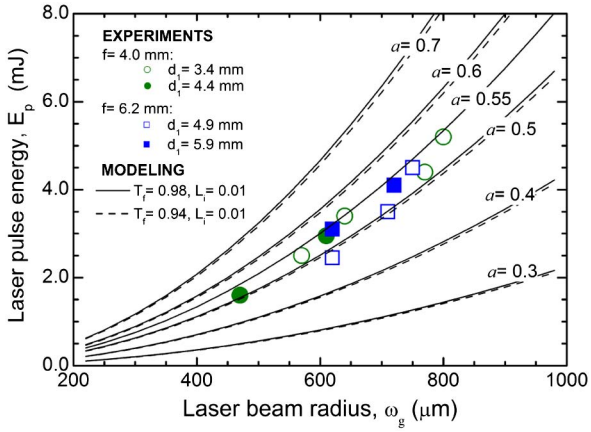

Fig. 3. Laser pulse energy E_p versus laser beam radius ω_g. Losses $L_i = 0.01$, and, for Cr^{4+}:YAG, final transmission T_f of 0.94 and 0.98 were considered in simulations.

Figure 3 presents modeling of laser pulse energy E_p function of laser beam radius ω_g; the value of ω_g was determined for each configuration by an ABCD formalism using the data recorded during M^2 factor measurements. In simulations, losses L_i were taken as 0.01 (a typical value for Nd:YAG with the doping level and length used in our experiments). Also, values of 0.94 and 0.98 for the final transmission T_f of Cr^{4+}:YAG were considered. One could observe that, for a fixed value of parameter a, the influence of total losses L_t on laser pulse energy is not too significant; more important is the value of a.

B. Four-Beam Output Laser

A typical laser module made in this work is shown in Fig. 4. The four prisms, P [Fig. 4(a)], were used to fold and redirect each pump beam from the corresponding optical fiber F toward the Nd:YAG/Cr^{4+}:YAG medium [Fig. 4(b)]. Several geometries were considered and realized. For example, a first one was built with identical aspherical lenses L of focal length $f = 4.0$ mm; distance d_1 was 3.4 mm and the Nd:YAG/Cr^{4+}:YAG medium was positioned at $d_2 = 8$ mm (we remember that, as shown in Fig. 1, on each folding arm, d_2 accounts for the distance from a lens L to Nd:YAG/Cr^{4+}:YAG). For a second arrangement (which will be discussed below) we used aspherical lenses with focal length $f = 6.2$ mm; distance d_1 was 4.9 mm and the distance d_2 was chosen as $d_2 = 15.5$ mm. Uncoated, 3 mm right-angle prisms were employed in this scheme, each prism being nearly 5 mm away from the corresponding lens L.

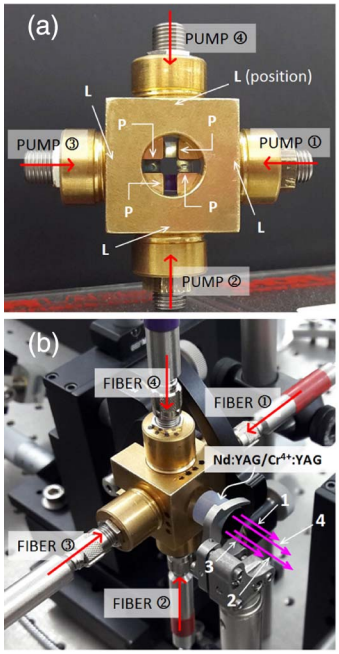

Fig. 4. (a) The module with the four folding prisms is presented. Each lens (L) position is indicated. P: prism. (b) A photo of the Nd:YAG/Cr^{4+}:YAG laser with four-beam output is shown. The directions of laser beams 1, 2, 3, and 4 are given by the colored lines with arrows.

At 5 Hz repetition rate, the laser pulse energies were 3.25 mJ for beam 1, 3.30 mJ for beam 2, 3.60 mJ for beam 3, and 3.20 mJ for beam 4. The small differences from the expected value of 3.4 mJ [according to Fig. 2(a)] could be attributed to some length differences in every pump line, as well as the fact that each pump was not made in the center of the Nd:YAG/Cr^{4+}:YAG medium but on its circumference (in this case, small differences in Nd concentration or coatings can affect the results). Moreover, differences in the four diode lasers used for pumping can influence the laser pulse energy. The pump pulse energies were 30.5 and 32 mJ for beams 1 and 2, respectively; E_{pump} amounted to 33 mJ for beam 3 and to 30 mJ for beam 4. Thus, the overall optical-to-optical efficiency (defined as the ratio between the laser pulse energy and the pump pulse energy, E_p/E_{pump}) was in the range of 0.103 for beam 2 up to 0.109 for beam 3. The pulse duration (which was determined with an ultrafast InGaAs photodetector, rise time shorter than 35 ps) was around 0.9 ns for each beam, and therefore the laser pulse peak power was in the range of 3.55 MW for beam 4 to 4.0 MW for beam 3.

Important for stable laser emission is the Nd:YAG/Cr^{4+}:YAG temperature. We have used an FLIR T620 thermal camera (−40°C to +150°C range, ±2°C accuracy) to measure the temperature of surface S2 of the Nd:YAG/Cr^{4+}:YAG medium. As shown in Fig. 5, when the laser medium was kept in air and with no cooling [as shown in Fig. 4(b)], after a few minutes of operation the maximum temperature of surface S2 at the location of beam 1 increases from 27°C at 2 Hz repetition rate up to 64.5°C at 60 Hz repetition rate. Similar results were recorded for all lines (and Fig. 5 presents also the temperature for the central axis of beam 4). Longer time operation could not be performed, especially at high repetition rate, as the medium temperature increased further and the laser

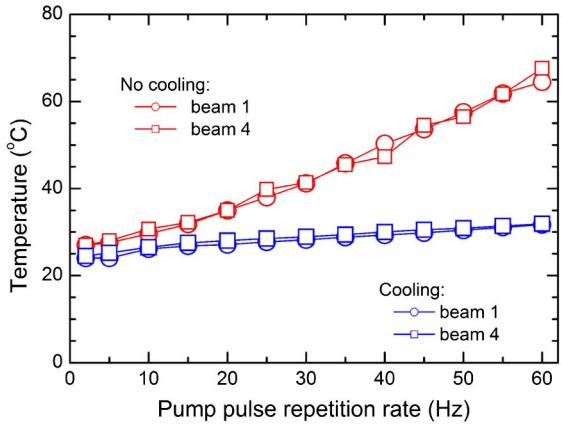

Fig. 5. Maximum temperature of surface S2 of Nd:YAG/Cr^{4+}:YAG at central locations of beams 1 and 4 versus the pump pulse repetition rate.

emission eventually ceased. Therefore, in the next experiments, the Nd:YAG/Cr^{4+}:YAG medium was wrapped in indium foil and then clamped in a copper holder; a fan was used to cool the metallic holder. The temperature of surface S2 was much lower in comparison with the previously described operation regime. Thus, as illustrated in Fig. 5, only a small increase in temperature, from 24.5°C at 2 Hz operation rate up to 30.8°C at repetition rate of 60 Hz was measured in the central position of beam 1. The laser pulse energy E_p was also stable at high rates of repetition. For operation at 60 Hz, the increase of E_p in comparison with the values measured at 5 Hz were below 3.7% for beams 1, 2, and 4; a slightly higher increase of 5.5% was measured for the energy of beam 3.

The laser device described in this work can be used (after further optimizations, testing, and integration) for multipoint ignition of an automobile engine, especially for ignition of lean air–fuel mixtures. Furthermore, it could be of interest for ignition of propellants in space applications or for ignition in turbulent conditions that are specific to aeronautics. For this purpose, different focusing schemes that allow access of a defined volume of fuel can be designed.

For example, as shown in Fig. 6(a), all beams could be focused in the same point; an aspherical lens with focal length of 8.1 mm (NA = 0.50) was used in this scheme. In another arrangement, each beam could be focused in a point on its axis of propagation, using identical lenses. Such a layout is presented in Fig. 6(b), where aspherical lenses with focal lengths from short, $f = 7.5$ mm (NA = 0.30), to long, $f =$ 18 mm (NA = 0.15), could be used to obtain air breakdown. We mention that the distance between the central axes of beams 1 and 3 and that between beams 2 and 4 was 7.0 mm. A larger volume could be accessed by focusing the beams at different distances from the optics. For example, Fig. 6(c) illustrates the air breakdown obtained with beams 1 and 3 from the horizontal plane that were focused in front of beams 2 and 4 (that are in vertical plane). A similar case is shown in Fig. 6(d), where beams 2 and 4 were focused close to the optics. Other combinations of optics could allow the focusing of each beam outside (or inside) its propagation axis, thus offering more possibilities for location of the ignition points in space. Furthermore, the timing between each beam could be controlled; in this way a method for avoiding misfiring, an event that usually happens in the case of igniting lean

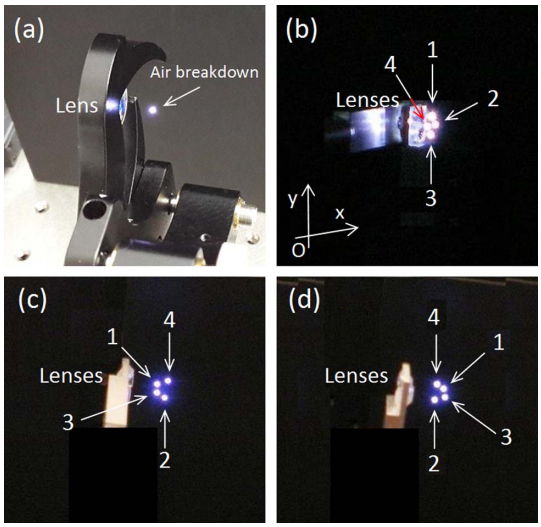

Fig. 6. Several combinations for focusing the laser beams are shown: (a) focusing in a single point; (b) focusing all beams in the same plane, at equal distances from the optics; (c) beams 1 and 3 (from the horizontal plane) are focused before beams 2 and 4 (from the vertical plane); (d) beams 2 and 4 are focussed close to the optics, in front of beams 1 and 3.

air–fuel mixtures, or for fuel in turbulent conditions. In addition, one more laser beam could be easily obtained by pumping the Nd:YAG/Cr^{4+}:YAG ceramic medium on its central axis. These approaches are under investigation and will be reported later.

3. CONCLUSION

We have proposed a high-peak-power passively *Q*-switched Nd:YAG/Cr^{4+}:YAG laser with four-beam output. Each pump line has a simple design, containing a lens and a folding prism. The laser yielded four beams, with energy per pulse of 3.25 mJ for beam 1, 3.30 mJ for beam 2, 3.60 mJ for beam 3, and 3.20 mJ for beam 4 at 5 Hz repetition rate. The pulse duration was about 0.9 ns. When the repetition rate was increased to 60 Hz, the laser pulse energy increased, in the range of 2.4% for beam 2 up to 5.5% for beam 3. Different focusing arrangements were presented to obtain air breakdown in variable volume. Some applications of such a laser device include ignition of lean air–fuel mixtures in automobile gasoline engines, ignition of a propeller under high-altitude conditions and even in space propulsion, or ignition in turbulent conditions that are specific to aeronautics.

Funding. Autoritatea Națională pentru Cercetare Stiințifică (ANCS) (PN-II-PT-PCCA-2011-3.2-1040 (58/2012), NUCLEU 4N/2016); Horizon 2020 (691688 LASIG-TWIN).

REFERENCES

1. P. D. Rooney, "Laser versus conventional ignition of flames," Opt. Eng. **33**, 510–521 (1994).
2. M. Weinrotter, H. Kopecek, and E. Wintner, "Laser ignition of engines," Laser Phys. **15**, 947–953 (2005).
3. J. Tauer, H. Kofler, and E. Wintner, "Laser-ignited ignition," Laser Photon. Rev. **4**, 99–122 (2010).
4. G. Dearden and T. Shenton, "Laser ignited engines: progress, challenges and prospects," Opt. Express **21**, A1113–A1125 (2013).
5. J. D. Dale, P. R. Smy, and R. M. Clements, "Laser ignited internal combustion engine: An experimental study," in *SAE International* (1978), paper 780329.
6. J. Mullett, P. Dickinson, A. Shenton, G. Dearden, and K. G. Watkins, "Multi-cylinder laser and spark ignition in an IC gasoline automotive engine: a comparative study," in *SAE International* (2008), paper 2008-01-0470.
7. H. Kofler, J. Tauer, G. Tartar, K. Iskra, J. Klausner, G. Herdin, and E. Wintner, "An innovative solid-state laser for engine ignition," Laser Phys. Lett. **4**, 322–327 (2007).
8. M. Tsunekane, T. Inohara, A. Ando, N. Kido, K. Kanehara, and T. Taira, "High peak power, passively *Q*-switched microlaser for ignition of engines," IEEE J. Quantum Electron. **46**, 277–284 (2010).
9. M. Tsunekane and T. Taira, "High peak power, passively *Q*-switched Yb:YAG/Cr:YAG micro-lasers," IEEE J. Quantum Electron. **49**, 454–461 (2013).
10. C. Y. Cho, H. P. Cheng, Y. C. Chang, C. Y. Tang, and Y. F. Chen, "An energy adjustable linearly polarized passively *Q*-switched bulk laser with a wedged diffusion-bonded Nd:YAG/Cr^{4+}:YAG crystal," Opt. Express **23**, 8162–8169 (2015).
11. T. Dascalu, G. Salamu, O. Sandu, M. Dinca, and N. Pavel, "Scaling and passively Q-switch operation of a Nd:YAG laser pumped laterally through a YAG prism," Opt. Laser Technol. **67**, 164-168 (2015).
12. G. Kroupa, G. Franz, and E. Winkelhofer, "Novel miniaturized high-energy Nd:YAG laser for spark ignition in internal combustion engines," Opt. Eng. **48**, 014202 (2009).
13. Y. Ma, X. Li, X. Yu, R. Fan, R. Yan, J. Peng, X. Xu, R. Sun, and D. Chen, "A novel miniaturized passively *Q*-switched pulse-burst laser for engine ignition," Opt. Express **22**, 24655–24665 (2014).
14. T. Taira, S. Morishima, K. Kanehara, N. Taguchi, A. Sugiura, and M. Tsunekane, "World first laser ignited gasoline engine vehicle," in *1st Laser Ignition Conference (LIC'13)*, Yokohama, Japan, (April 23–25, 2013), paper LIC3-1.
15. N. Pavel, T. Dascalu, G. Salamu, M. Dinca, N. Boicea, and A. Birtas, "Ignition of an automobile engine by high-peak power Nd:YAG/Cr^{4+}:YAG laser-spark devices," Opt. Express **23**, 33028–33037 (2015).
16. T. X. Phuoc, "Single point versus multi-point laser ignition: Experimental measurements of combustion times and pressures," Combust. Flame **122**, 508–510 (2000).
17. M. Weinrotter, H. Kopecek, M. Tesch, E. Wintner, M. Lackner, and F. Winter, "Laser ignition of ultra-lean methane/hydrogen/air mixtures at high temperature and pressure," Exp. Therm. Fluid Sci. **29**, 569–577 (2005).
18. N. Pavel, M. Tsunekane, and T. Taira, "Composite, all-ceramics, high-peak power Nd:YAG/Cr^{4+}:YAG monolithic micro-laser with multiple-beam output for engine ignition," Opt. Express **19**, 9378–9384 (2011).
19. E. Lyon, Z. Kuang, H. Cheng, V. Page, A. T. Shenton, and G. Dearden, "Multi-point laser spark generation for internal combustion engines using a spatial light modulator," J. Phys. D **47**, 475501 (2014).
20. Y. Ma, Y. He, X. Yu, X. Li, J. Li, R. Yan, J. Peng, X. Zhang, R. Sun, Y. Pan, and D. Chen, "Multiple-beam, pulse-burst, passively *Q*-switched ceramic Nd:YAG laser under micro-lens array pumping," Opt. Express **23**, 24955–24961 (2015).
21. C. Manfletti and G. Kroupa, "Laser ignition of a cryogenic thruster using a miniaturised Nd:YAG laser," Opt. Express **21**, A1126–A1139 (2013).
22. C. Manfleti and M. Börner, "Laser ignition systems for space propulsion applications," in *4th Laser Ignition Conference (LIC'16)*, Yokohama, Japan, (May 18–20, 2016), paper LIC6-3.
23. L. Zimmer, R. George, and M. Orain, "Laser ignition in an aeronautical injector," in *2nd Laser Ignition Conference (LIC'14)*, Yokohama, Japan, April 22–24, 2014, paper LIC3-6.
24. J. J. Degnan, "Theory of the optimally coupled Q-switched lasers," IEEE J. Quantum Electron. **25**, 214–220 (1989).
25. J. J. Degnan, "Optimization of passively Q-switched lasers," IEEE J. Quantum Electron. **31**, 1890–1901 (1995).